Assessment of Clinical Guidelines Used to Predict Impending Fracture of Bones with Metastatic Defects

by

Robyn Lee Jaloszynski

Submitted to the Department of Mechanical Engineering
in partial fulfillment of the requirements for the degree of

Bachelor of Science in Mechanical Engineering

at the

MASSACHUSETTS INSTITUTE OF TECHNOLOGY

June 1991

Author .. ..
Department of Mechanical Engineering
May 10, 1991

Certified by .....
Wilson C. Hayes, Ph.D.
Maurice E. Mueller Professor of Biomechanics, Harvard Medical School and Harvard/MIT Program in Health Sciences & Technology
Thesis Supervisor

Accepted by ....
Peter Griffith
Professor of Mechanical Engineering and Chairman, Departmental Committee

Assessment of Clinical Guidelines Used to Predict Impending Fracture of Bones with Metastatic Defects

by

Robyn Lee Jaloszynski

Submitted to the Department of Mechanical Engineering
on May 10, 1991, in partial fulfillment of the
requirements for the degree of
Bachelor of Science in Mechanical Engineering

Abstract

Pathological fracture due to osseous metastatic defects has become more common due to the increasing longevity of cancer patients. Thus, there is an increasing need to determine when a defect poses a significant fracture risk. However, currently there are only limited, qualitative guidelines to indicate when pathologic fracture of the femur is iminent, namely: 1) the lesion involves more than 50% of the cortex, 2) it is greater than 2.5 cm in diameter, or 3) the lesion is very painful and unresponsive to radiation therapy. Recent research has indicated that following the 50% cortical loss criterion would lead to extensive reduction in both bending and torsional strength. From this research, it seems that this would allow advancing defects to reach unacceptable levels of risk long before the geometric criteria for impending fracture are met. In addition, because of the difficulty in determining the reduction in cross-sectional area, it is suspected that clinicians do not follow the geometric criteria. Also, pain often seems to supercede the use of the geometric bone loss requirement.

The purpose of this study was to assess the current criteria for impending fracture and compare them to new information concerning the biomechanical behavior of femoral defects. In addition, the question of whether the geometric criteria are being followed by clinicians was also addressed. A population of thirteen patients with osseous defects of the femur were included in the study, all of whom had been described clinically as having impending fracture. Quantitative computed tomography scans were analyzed with previously developed techniques, yielding values for cortical bone loss and strength reduction. Support for the strength reduction calculations for an endosteal, diaphyseal defect came from comparison to predictions employing finite element models and experimental results. It was also found that there was no universal correlation between reduction in cross-sectional area and strength reduction which was applicable to all types of defects (as the current criteria presume). In addition, it was determined that the average percentage of cortical bone remaining in these cases was 93% (well above the 50% criterion value) and therefore, that the guideline was not being used to assess these lesions. From these observations, it seems clear that the current 50% cortical loss guideline is unsubstantiated, inappropriate, hazardous.

and impractical. Additional research will be required, however, to determine more appropriate clinical guidelines for the treatment of osseous defects.

Thesis Supervisor: Wilson C. Hayes, Ph.D.
Title: Maurice E. Mueller Professor of Biomechanics, Harvard Medical School and Harvard/MIT Program in Health Sciences & Technology

Acknowledgments

I would like to thank Dr. John Hipp for his patience and help and Dr. Dempsey Springfield of Massachusetts General Hospital for his clinical support of this project. Thanks also to my family and my best friend, John Gilbert, for their continued support and encouragement. Finally, I would like to mention the International Union of Operating Engineers for the four years of extensive financial support they have given me as a National Merit Scholar.

This research was supported by a grant from the National Institute of Health and was performed at the Orthopaedic Biomechanics Laboratory, Department of Orthopaedic Surgery, Charles A. Dana Research Institute, Beth Israel Hospital, Boston.

Contents

List of Figures

Chapter 1

Introduction

1.1 Significance

More than one-third of the approximately 930,000 new cases of cancer diagnosed in 1983 were predicted to be bone-seeking malignant tumors of the breast (123,000), lung (144,000), and prostate (75,000) [27]. Approximately 50% of these patients will have metastasis to bone during the course of their treatment [20] with the femur being one of the most frequent and dangerous sites because of its load-bearing function. In a study of 2000 patients with metastatic bone disease, 25% had lesions in the femur [28]. When only breast and prostate cancer are considered, the number is even more significant. For metastases from breast cancer, lesions are found in the femur 54% of the time; for prostate cancer, 68% of the time [10, 18].

In the last decade, there have been significant improvements in treatments for cancer, resulting in increased longevity for patients. Unfortunately, as the patients live longer with the disease, the number and extent of their metastases and resulting pathological fractures also increases. Prophylactic stabilization of serious defects is thus required more and more often since it has several advantages over treating any subsequent pathological fracture. These advantages include: relief of pain, decreased hospital stay, reduced operative difficulty, reduced risk of non-union, and reduced morbidity. Prophylactic stabilization has been suggested as the most favorable treatment for lesions that are advancing, are resistant to other treatment, or are already

likely to cause pathologic fracture [1, 2, 6, 8, 12, 19, 24, 26, 29]. The femur alone accounts for approximately 61% of all long-bone pathological fractures [13, p.141] which is one of the reasons it has been chosen for the emphasis of this study. In addition, the roughly tubular shape of the femur lends itself more readily to mechanical analysis.

1.2 Background

With the increasing frequency of osseous metastases, the development of guidelines for appropriate management is essential for the patient's care. Most commonly, the size, location, and appearance of the defect dictate the method of treatment, along with the individual's degree of pain and physical activity. Since the prevention of fracture is an immediate goal of any clinical management, the ideal information would be an objective assessment of the **fracture risk** based on the particular defect and patient involved. Unfortunately, there are no established biomechanical guidelines to relate the defect characteristics to a reduction in bone strength (or "fracture risk"). However, there has been previous work done to establish qualitative guidelines and recently, there has been improvement in techniques to predict the biomechanical properties of bones with defects.

Three general criteria have been proposed to indicate when fracture of the femur is iminent due to metastatic defects, namely: 1) the lesion involves more than 50% of the cortex, 2) it is greater than 2.5 cm in diameter, or 3) the lesion is very painful and unresponsive to radiation therapy [2, 8]. These guidelines, however, were either subjective or derived from clinical experience involving very few cases and have not been scientifically validated [6, p.173]. Furthermore, the 2.5 cm diameter criterion is inherently inappropriate for universal application since it is not normalized in any sense. Obviously, a 2.5 cm defect will pose a much greater fracture risk in a bone with a nominal size of 3 cm than in one with a diameter of 5 cm.

Subsequent research attempted to determine the relationship between the biomechanical properties of the bone and the geometric characteristics of the lesion. In

1959, Bechtol [3] studied the effect of screw holes on breaking strength by testing paired bones in three-point bending. He examined holes which were between 3% and 40% of the diameter of the bone. His conclusions were that holes less than 20% of the diameter of the bone caused a 40% decrease in strength, while holes larger than 20% decreased the strength linearly with hole size. The variation in breaking strength for his experiments however, was reportedly about 15%.

Six years later, Frankel and Burstein [9] found that a single saw cut of one-fifth the length of of the tibia decreased the torsional energy absorption by 70% in three pairs and that increasing only the width had no effect. In 1970, Brooks et al. expanded on the research conducted by Bechtol; testing pairs of canine femora in torsion with circular defects smaller and larger than the 20% suggested by Bechtol [4]. They found that holes with diameters of 12% to 28% of the bone diameter caused the same decrease of 55% in energy absorption until failure occurred. Thus, these results failed to establish the transition point between small, "stress-riser" defects and larger, "open-section" defects that Bechtol's study had indicated.

Different findings concerning the effect of defect width (perpendicular to the bone axis) and length were reported by Clark et al. in 1977 [7]. For defects ranging from 9% to 17% of the cross-sectional area of the bone, an oval shape was found to be stronger than a rectangle in pairs of human femora. Increasing the width caused a statistically significant decrease in strength, while increasing the length did not. This, in effect, contradicted the work of Frankel and Burstein.

More recently (1984), McBroom and Hayes of the Orthopaedic Biomechanics Laboratory (Beth Israel Hospital) studied the weakening effect of drilled holes (10% to 50% of bone diameter) in paired canine femora using four-point bending [22]. They found that bending strength decreased most rapidly as the size of the defect approached 20%. At more than 20%, the decrease in bending strength versus hole size approached a linear relationship. Later, in 1986, McBroom et al. [23] directed their attention to the analysis of endosteal defects, simulating them in canine femora which were tested in four-point bending. Their results indicated that the length of a defect did not influence the flexural strength, but that strength reduction was linearly

related to reduced cortical area caused by endosteal defects. For these defects, the bending strength decreased by nearly 55% when the defect diameter approached 50% of the intact cortical diameter.

In an attempt to assess the established criteria of 50% cortical bone loss, Leggon et al. [17] tested an oblong defect configuration involving 50% of the canine femoral diaphysis in torsion to determine the strength reductions incurred and the benefits of certain internal fixation methods. The femurs with a 50% cortical loss demonstrated only a $12.7 \pm 3.8\%$ of intact bone strength, suggesting that lesions should not be allowed to progress to this state.

Several recent studies conducted at the Orthopaedic Biomechanics Laboratory of Beth Israel Hospital have explored the biomechanics of diaphyseal osseous metastatic lesions and have cast further doubt on the 50% cortical loss guideline [21, 15, 16]. These analytical and experimental studies have demonstrated that diaphyseal transcortical defects involving 50% cortical loss involve 80-90% reductions in bone bending strength. Endosteal defects involving 50% cortical loss incur a 60-70% reduction. It was also found that the length of a transcortical defect along the bones' long axis strongly influenced the torsional strength, while for an endosteal defect, the length had little effect on the bone bending strength. For endosteal defects, the results indicated that the minimum wall thickness and its location with respect to the bending loads are the most critical aspects of the defect geometry. Since one of the cases in the present study involves an endosteal, diaphyseal defect, comparison was possible with the strength predictions of the study of Hipp, et al. (concerning endosteal lesions) [16] and will be presented later in more detail.

Unfortunately, there are still some uncertainties associated with these results. First of all, the reduction in the quality of the bone surrounding the defect could have an unknown (positive or negative) influence on bone strength depending on whether there are stress concentrations around the defect. Further uncertainties result from the lack of data on the morphological features and biomechanical properties of bone surrounding metastatic lesions.

1.3 Current Objectives

Recent research has indicated that following the 50% cortical loss criterion would lead to extensive reduction in both bending and torsional strength. From these studies, it seems that this would allow advancing defects to reach unacceptable levels of risk long before the criteria for impending fracture is met. In addition, the "traditional" guidelines do not reflect the recent, pertinent research regarding the structural behavior of bones with defects. Furthermore, because of the relatively low incidence of pathological fracture (in patients with known lesions) and the difficulties associated with radiographic assessment of cortical loss, it is suspected that clinicians do not follow the geometric criteria in determining which defects suggest impending fracture. Rather, the pain associated with microfractures at the defect becomes so great as to commonly supercede the use of the geometric bone loss requirements.

The purpose of this study was to assess the current clinical guidelines for determining impending fracture and compare them to new information concerning the biomechanical behavior of femoral defects. In addition, the question of whether the geometric criteria are being followed by clinicians was also to be answered. Particular attention was paid to the 50% cortical loss criterion as the '2.5 cm diameter' criterion has already been deemed inappropriate for application to every size of femur. The cortical loss guideline will be discounted by: 1) noting that it is not scientifically validated, 2) demonstrating that the strength reduction associated with a 50% reduction in cortical area is substantially higher than what would pose "acceptable" fracture risk, 3) showing that there is no correlation between cortical area loss and strength reduction when a range of defect types is considered, (if it is possible to define such a cortical loss criterion, it most likely will be different for each type of defect rather than universal, like the current guidelines) and 4) introducing the idea that the criterion is not being employed rigorously anyway (since it is difficult to get a true measure of cortical area and pain or other factors often preclude the use of the criterion).

Chapter 2

Methods and Theory

To address these goals, quantitative computed tomography (QCT) scans were obtained in the routine course of clinical care of patients exhibiting established defects of the femur. Patients were included who were identified (through a positive bone scan and/or plain radiography) to have established defects which raised in the mind of the radiologist a risk of pathologic fracture. Most of these were metastases, but several cases of primary bone tumors and benign conditions (such as non-ossifying fibromas) were also included as they pose similar fracture risks and may be analyzed in the same way. Several collaborating clinicians from Massachusetts General Hospital provided the primary source of referral for patients to this study, including Drs. Dempsey Springfield, Henry Mankin and Fred Mansfield from the Orthopaedic Oncology Service and Dr. Joanna Sawicka from the Breast Cancer Clinic.

2.1 Patient Population

Thirteen patients were chosen from among the entire collection of clinical QCT scan data at the Orthopaedic Biomechanics Laboratory. The criteria for inclusion were: 1) the presence of an established, osseous defect located in the femur which had been described as having an impending fracture, and 2) the availability of a QCT scan which included both the pathologic bone and the contralateral femur. Seven of the patients were female, the rest male. Ages ranged from 5 to 78 years, with the average

being approximately 45.3 years (SD = 26.8). A significant range of lesion types and locations was represented. A summary of patient characteristics is included in Appendix A.

2.2 Computed Tomography Scanning Procedure

Computed tomography was chosen for the defect imaging because it allows more accurate and easier measurement of bone crossections than conventional radiographs. Plane radiographs could also have been misleading in that an asymmetric defect may not appear to require treatment if the radiograph is not taken in the proper orientation. In addition, because of its ability to define clearly and supply accurate density measurements for small volumes of tissue, QCT was especially suited for this study. All QCT scans were acquired as part of the routine course of clinical care of patients with metastatic bone disease using a GE9800 scanner. It should be noted that no new methods of assessment beyond obtaining QCT scans according to a previously established, standard protocol were imposed.

Special polyethylene phantoms containing chambers of various concentrations of dibasic potassium phosphate were included in the scan field to provide calibration for each scan and eliminate the effect of time-related scanner drift. Genant et al. reported that the precision for measurements using such phantoms at their institution has been approximately 2% [11]. Overall scout views were used to locate the bone lesions and then the region of the defect was scanned at 3.0 mm intervals. Magnetic tapes were used to store the QCT information and transfer it to the Orthopaedic Biomechanics Laboratory.

Typical scans and scout views can be seen in Figures 2-1 through 2-4. Figure 2-1 illustrates a typical crossectional image from one CT slice. The picture shows a defect in the right proximal femur and includes the five-chambered phantom placed underneath the patient. Figure 2-2 is a complete scout view of the same patient, while Figure 2-3 is a magnified subimage of the area containing the defect. Figure 2-4 is a similar subimage of a scout view for a different patient.

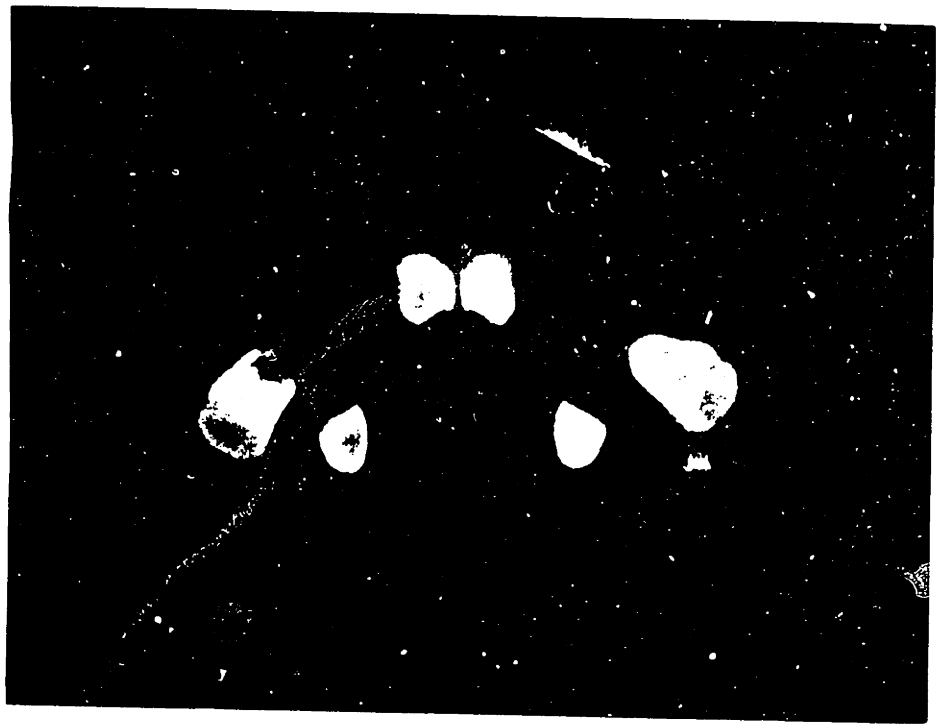

Figure 2-1: CT image in region of proximal femur for patient G.L. (9 yr. old male) which includes a five-chambered, dipotasium phosphate phantom. Note "open" defect in right femur.

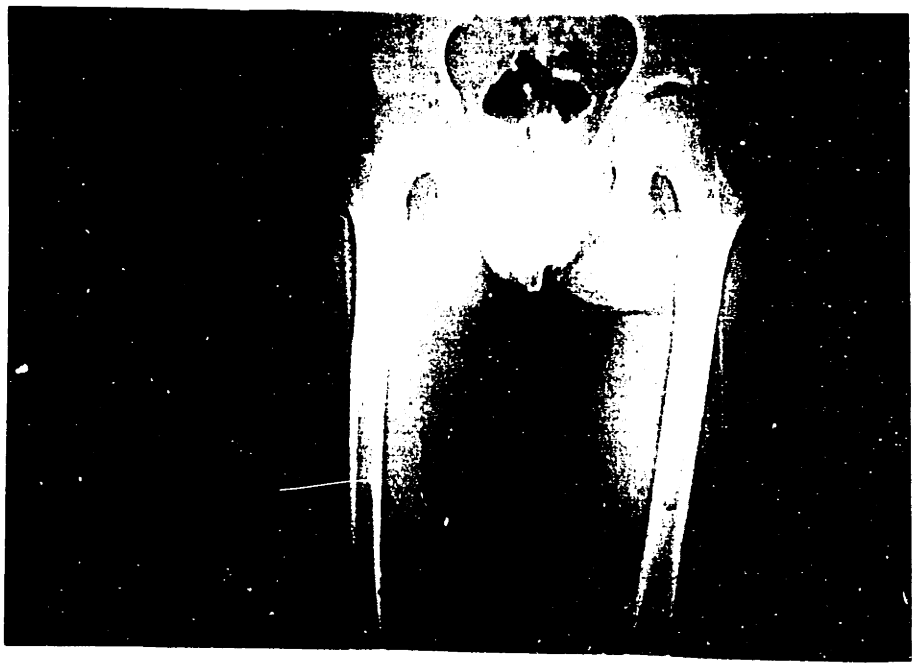

Figure 2-2: Example of complete scout view; patient, G.L. (9 yr. old male).

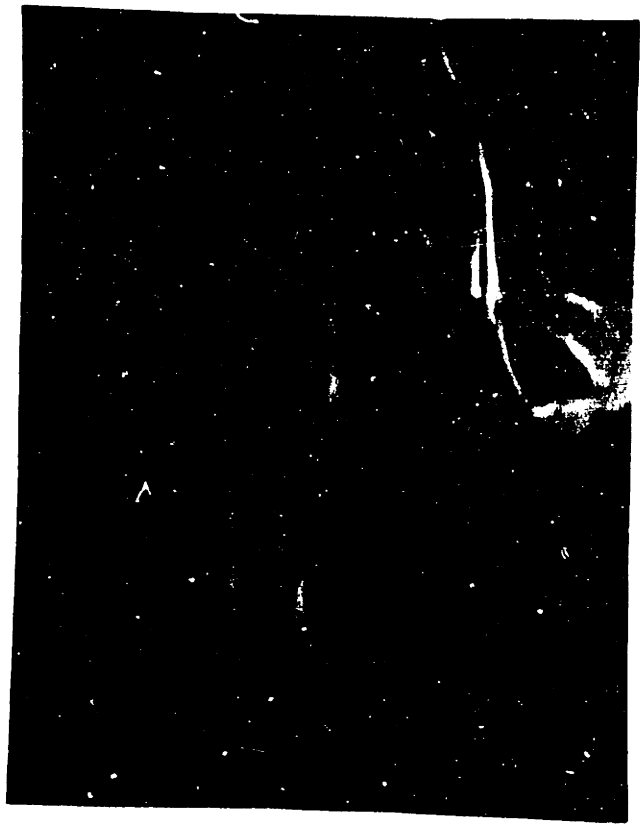

Figure 2-3: Magnified subimage of scout view in Figure 2-2, showing area of defect.

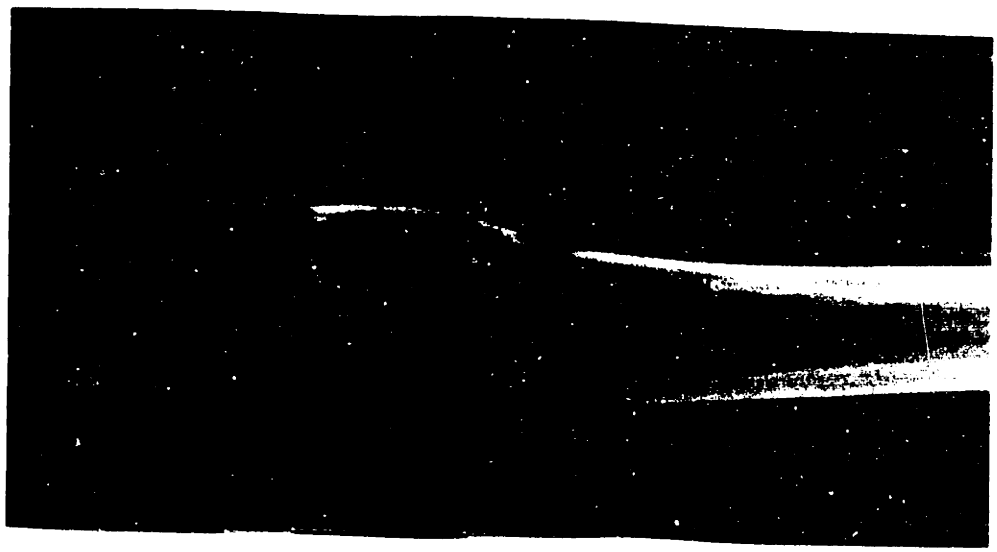

Figure 2-4: Example of a magnified subimage of a scout view for patient D.J., a 5 yr. old male. Defect is located in the distal left femur.

2.3 Image Processing and Analysis

After being read by the laboratory's VAX 11/750 system, a GOULD FD 5000 image processing system was used to identify lesion margins and estimate local densities and mechanical properties of the bone within and around the lesion. For each scan interval, subregions enclosing the image of each bone's crossection were defined and stored. For one of the images, additional subregions were defined which included the crossectional images of the five phantom chambers.

In the display, the reconstructed CT slice was regarded as a two-dimensional matrix of picture elements, or pixels. The computer displayed the array of pixels on a video monitor using varying shades of gray to represent the computed tomography numbers. For the GE9800 scanner, the CT number was recorded in Hounsfield units + 1000 (thus, water=1000). As part of the analysis, these CT numbers were converted to density values using the phantom data and an empirically derived relationship between dipotassium phosphate density and bone density. Each pixel was then assumed to represent bone if the density was above a threshold value of 160 mg/cm^3. The bone's modulus of elasticity was determined using the Carter-Hayes relation of Modulus = 3790 x $(Density)^3$ [5] (Figure 2-5). This relationship indicates that subtle changes in bone density result in large differences in modulus.

To determine the structural properties of the bone, two geometrical aspects must also be analyzed: the crossectional area and moment of inertia. The crossectional area for each slice was determined by counting the number of pixels which were above the density-threshold and therefore represented bone. The moment of inertia expresses the shape of the series of crossections and their distribution with respect to applied bending loads and a particular axis (i.e. area which is farther from the axis is more effective at resisting bending with respect to that axis). For this study, the moment of inertia was calculated by analyzing the crossectional slices together as a series; a method which will be described later.

Two types of loading were considered for the strength analysis: axial loading and bending. In each case, the behavior of the structural bone was described by a rigidity

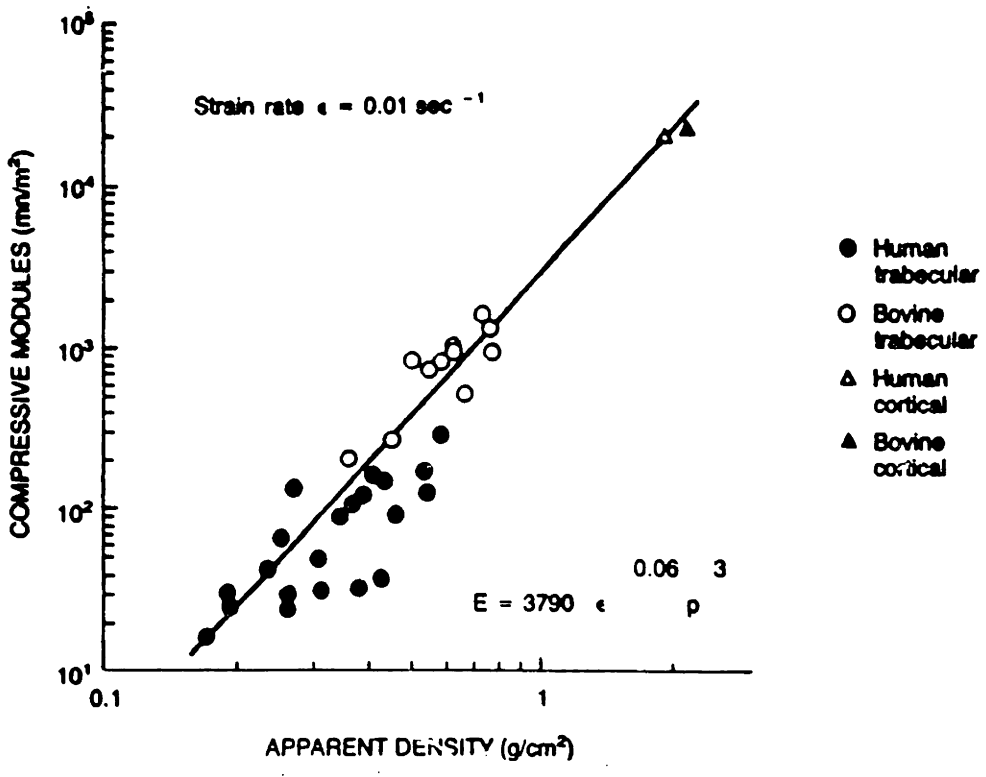

Figure 2-5: Modulus as a function of apparent density for human and bovine trabecular and cortical bone. Adapted from Carter and Hayes, 1977. [5]

term which is a combination of material stiffness (represented by the modulus) and a geometric factor (area or moment of inertia). For axial loading, the rigidity was determined by the product of the crossectional area and the modulus of elasticity (Figure 2-6). In bending, the product of the elastic modulus and the moment of inertia is the bending (or flexural) rigidity (Figure 2-7) which was calculated for the directions of maximum and minimum stiffness (expressed as maximum and minimum bending rigidity). For comparison among cases, the values for the pathologic sides were normalized to equivalent scans of the contralateral, normal femurs.

Each cross-section was considered to be a composite beam, with each pixel representing a component of the beam and having its own density and elastic modulus. Using this concept, the moment of inertia and rigidity were determined for each scan using the following equations for composite beam theory [25].

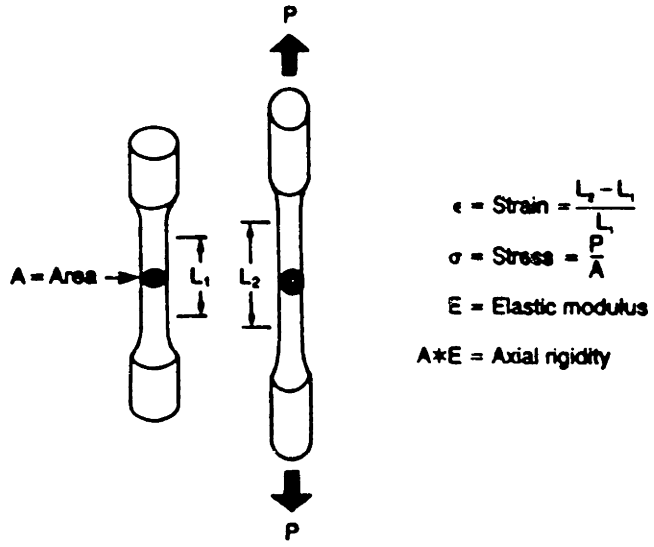

Figure 2-6: Representation of simple uniaxial tension test used to define axial rigidity. Adapted from Hipp, et al. 1991. [14]

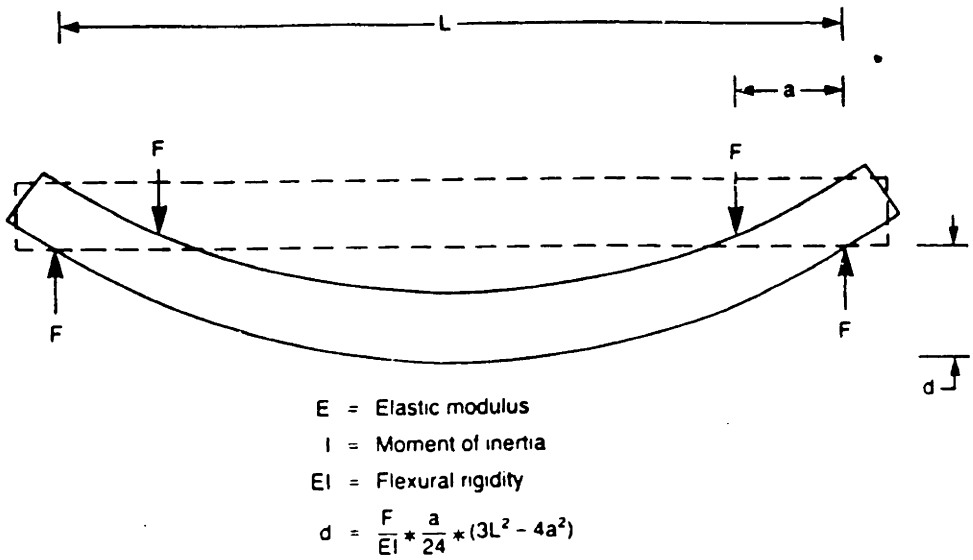

Figure 2-7: Representation of four point bending of a beam used to define bending rigidity. Adapted from Hipp, et al. 1991. [14]

The x-coordinate of the modulus-weighted neutral axis, x, was given by:

$$x = \frac{\sum_1^n x_i E_i A_i}{\sum_i^n E_i A_i}$$

where:

x_i is the coordinate of the centroid of the i^{th} pixel,

A_i is the area of the i^{th} pixel, and

E_i is the elastic modulus of the i^{th} pixel.

Once the location of the modulus-weighted neutral axis was known, the modulus-weighted rigidity, EI, could be determined from:

$$EI = \sum_i^n x_i^2 E_i A_i$$

where:

x_i is the distance from the modulus-weighted neutral axis to the i^{th} pixel.

The moment of inertia, I, was computed from:

$$I = \sum_1^n x_i^2 A_i$$

and E_{avg} was given by:

$$E_{avg} = \frac{1}{n} \sum_1^n E_i$$

As previously described, the elastic modulus for each pixel was determined from the Carter-Hayes relationship: $E = 3790 \text{ x } \rho^3$.

In order to partially substantiate the strength reductions calculated using this composite beam analysis, the value for an endosteal, diaphyseal defect (patient A.B.) was compared to predictions employing finite element analysis and experimental results reported by Hipp, et al. in "Structural Consequences of Endosteal Metastatic Lesions in Long Bones" [16]. Since the defect in patient A.B. was a real example of the type that Hipp et al. attempted to replicate, it was hoped that the strengths predicted in both studies would agree. The graph in Figure 2-8 (taken from "Structural

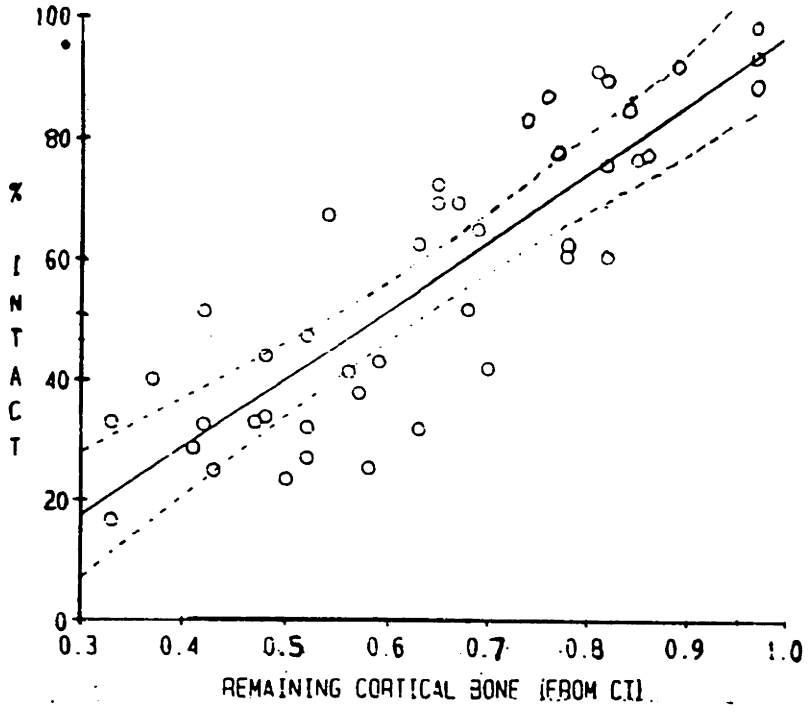

Figure 2-8: Percent intact strength as a function of percent cortical bone remaining (determined by CT). % Intact Strength = (114 x % remaining cortical area) - 16.7 where R^2=0.738. Adapted from Hipp, et al., 1989. [16]

Consequences...") shows the experimental data for canine femurs loaded to failure in four point bending. The percent of contralateral intact bone strength is shown as a function of the ratio of compromised bone area to intact bone area as measured by CT scans through the defect. The linear regression line and 95% confidence intervals for the data are also shown. In addition, finite element models (linear and non-linear, not shown in figure) had been found to agree with the experimental data, with nearly all of the model-generated points falling within the 95% confidence interval. The bending rigidities predicted in the present study were plotted on the same graph as in Figure 2-8 in order to determine if the values are statistically similar (to be presented with the other results in Chapter 3).

2.4 Three Dimensional Reconstruction

Additional information concerning the lesion geometry was acquired using three dimensional reconstructions of the volume surrounding the defects. In fact, this was often the only way to truly appreciate the extent and geometry of the lesions or observe actual bone density distribution. Reconstructed volumes were created using the volume rendering component, SunVoxel, of SunVision software (Sun Microsystems, Inc.). which generated images from the volumetric data supplied by the CT scan. The volume data was the series of slices taken together, with each slice representing a two-dimensional array of density values. The CT data was changed to volume data by giving each image a thickness or 'length' of 3 mm corresponding to the interval between crossectional images. The volume elements are called *voxels* – the volumetric equivalent of the two-dimensional pixel.

The basic *texture mapping* mode mapped volume data values onto the surface of the volume, which was treated as a three-dimensional cube. The "block" may be sliced at any angle to display the data values of the exposed slice as well as the values of the unsliced faces (Figure 2-9); it may also be magnified or rotated. In order to "smooth" the figure, a trilinear interpolation mapping function was employed. In *transparent surfaces* rendering mode, the figure was modified using a set of substance classification properties. Ranges of density values were defined and each range was then given a color and an opacity value. In this way, non-essential portions of the volume such as skin and muscle could be made transparent, leaving only the image of the bone. Furthermore, the variation of density within the bone could be made more apparent. For the reconstructions in this study, the color-coding is such that normal cortical bone appears yellow-white, and trabecular bone appears blue-purple. Examples of three-dimensional reconstructions created using these techniques are shown in Figures 2-10 through 2-13.

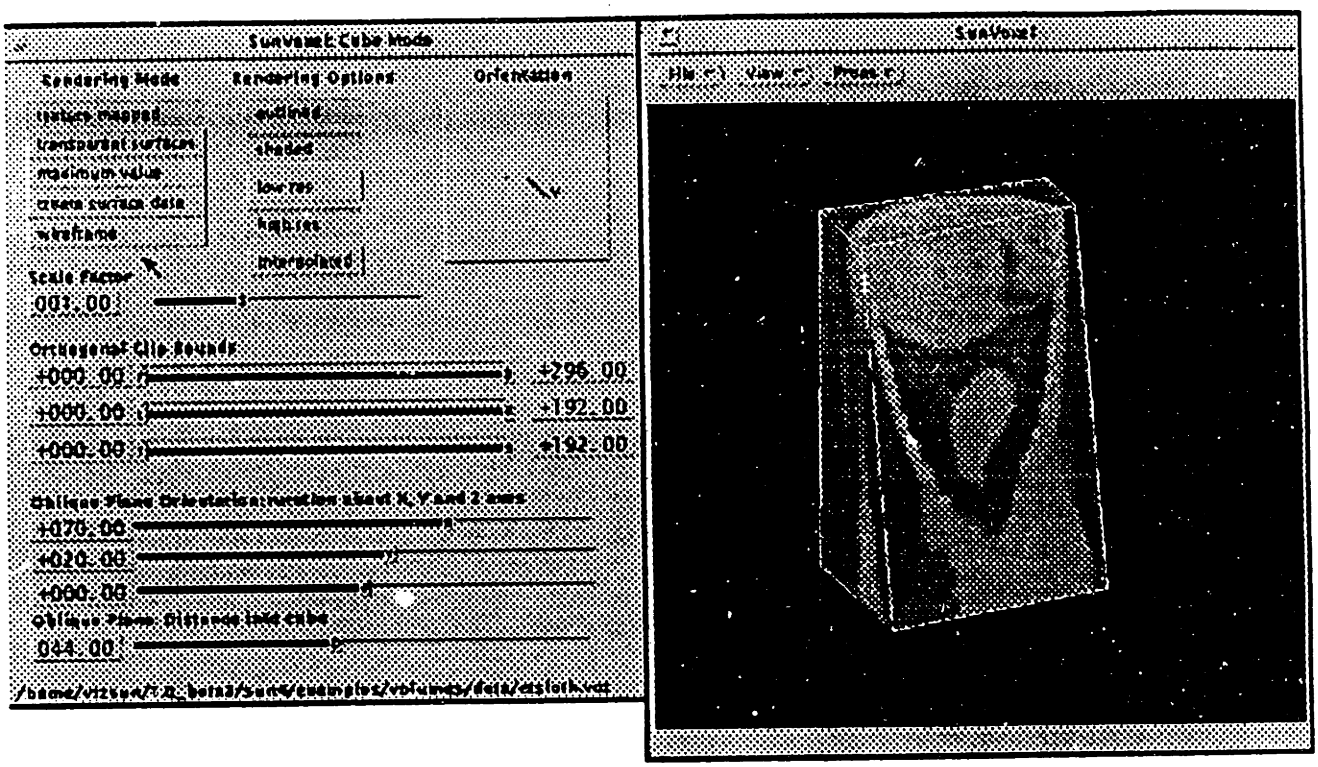

Figure 2-9: SunVoxel menu and example figure, demonstrating the ability to "slice" into a figure to expose an inner section.

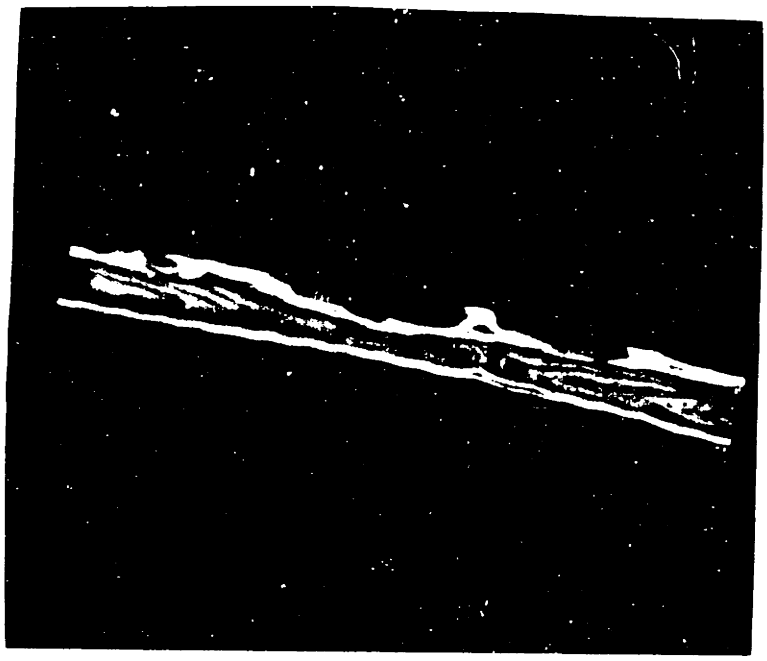

Figure 2-10: Typical color three-dimensional reconstruction for 12 yr. old patient with metastatic defect in the diaphysis of the left humerus. A large lesion was located on the lateral aspect, with extensive bone remodelling evident. There are several lesions present in various locations, with narrowing of the medullary canal and a layer of bone lateral to the voids. (This patient was not used for the study as defect was not in the femur.)

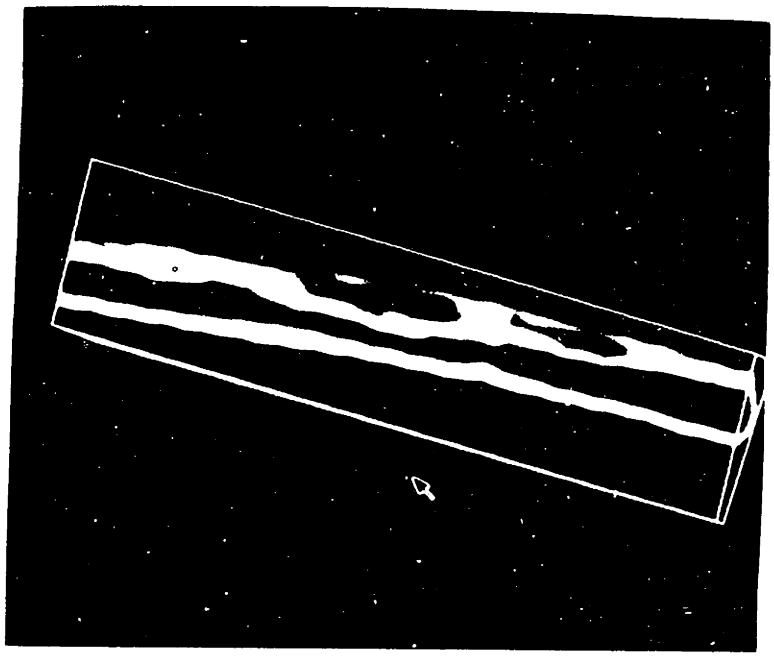

Figure 2-11: Black and white reconstruction analogous to that of Figure 2-10.

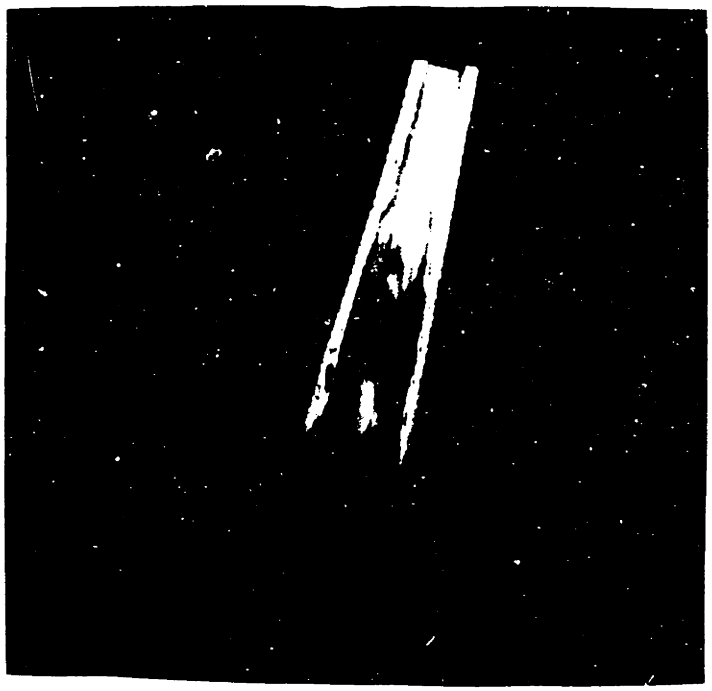

Figure 2-12: Typical color three-dimensional reconstruction for female, 12 yr. old patient with a defect in the distal left femur. The anterior third of the bone has been removed to visualize the interior of the femur. A perforation through the posterior wall can be seen above the metaphysis, along with increased bone density around the proximal border of the perforation. There is also erosion of the endosteal wall in several places.

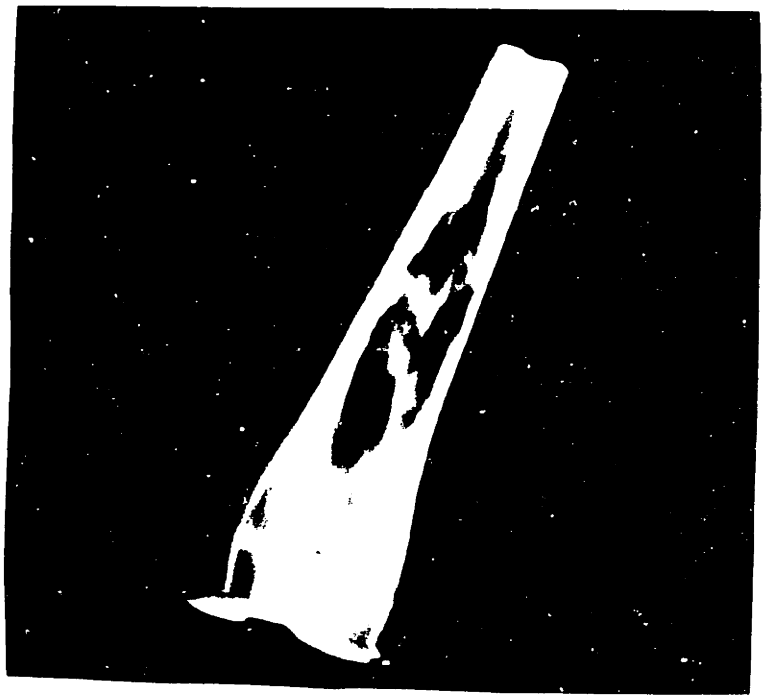

Figure 2-13: Black and white reconstruction analogous to that of Figure 2-12.

Chapter 3

Results

3.1 Representative Graphs

Figures 3-1 through 3-5 show some representative plots for patient L.R. (a 77 yr. old male, defect in right femoral diaphysis) resulting from the previously described biomechanical analysis. Figures 3-1 and 3-2 illustrate the changes in density and modulus with scan location; showing the difference between the pathologic and normal sides in the region of the defect. Figure 3-3 illustrates the reduction in cortical crossectional area over the area of the defect. Like the remaining graphs, the values for the pathologic bone have been normalized with respect to the contralateral, normal side. This was done in order to see the percentage of reduction more easily and enable comparison among cases. Similarly, Figures 3-4 and 3-5 show the reduction in strength, both axial and bending, by plotting the normalized values for axial and bending (maximum and minimum) rigidities.

These type of plots were created for all thirteen patients in the study, yielding values of crossectional area, density, modulus, axial, and bending rigidity for each scan location. The values of greatest interest are the minimum values which are located in the regions of the defects. These are the points of highest fracture risk and thus are the values which should be assessed in relation to the fracture risk criteria. In the previous normalized plots (Figures 3-3 through 3-5), these values appear as the 'valleys' of the curves. A summary of these minimum values for all of the cases is

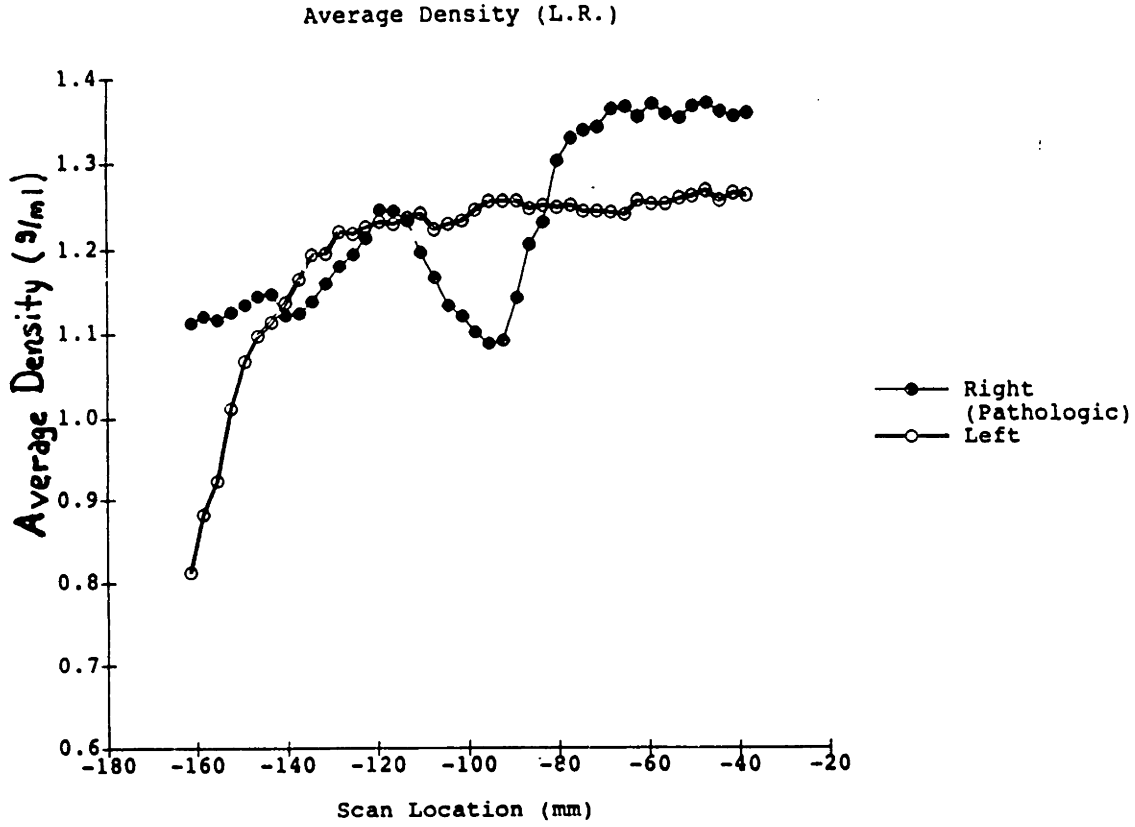

Figure 3-1: Change in average density with scan location for both pathologic and normal sides.

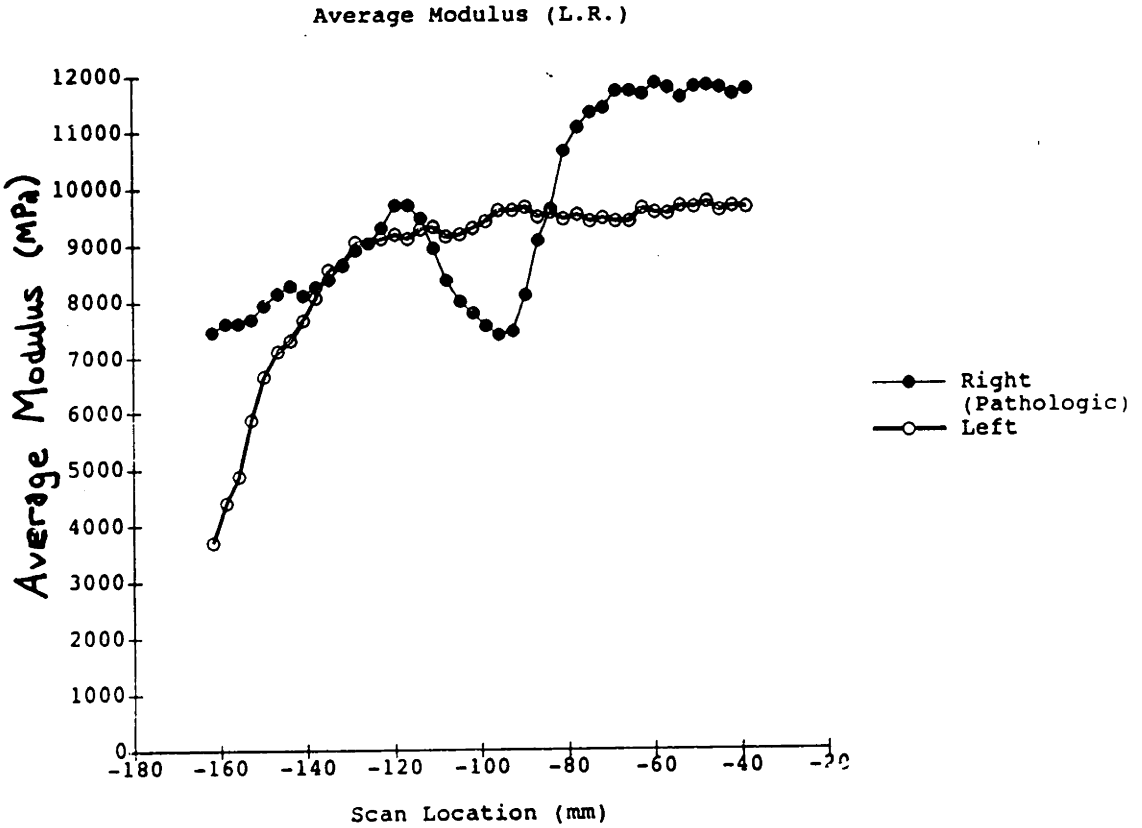

Figure 3-2: Change in average modulus with scan location for both pathologic and normal sides.

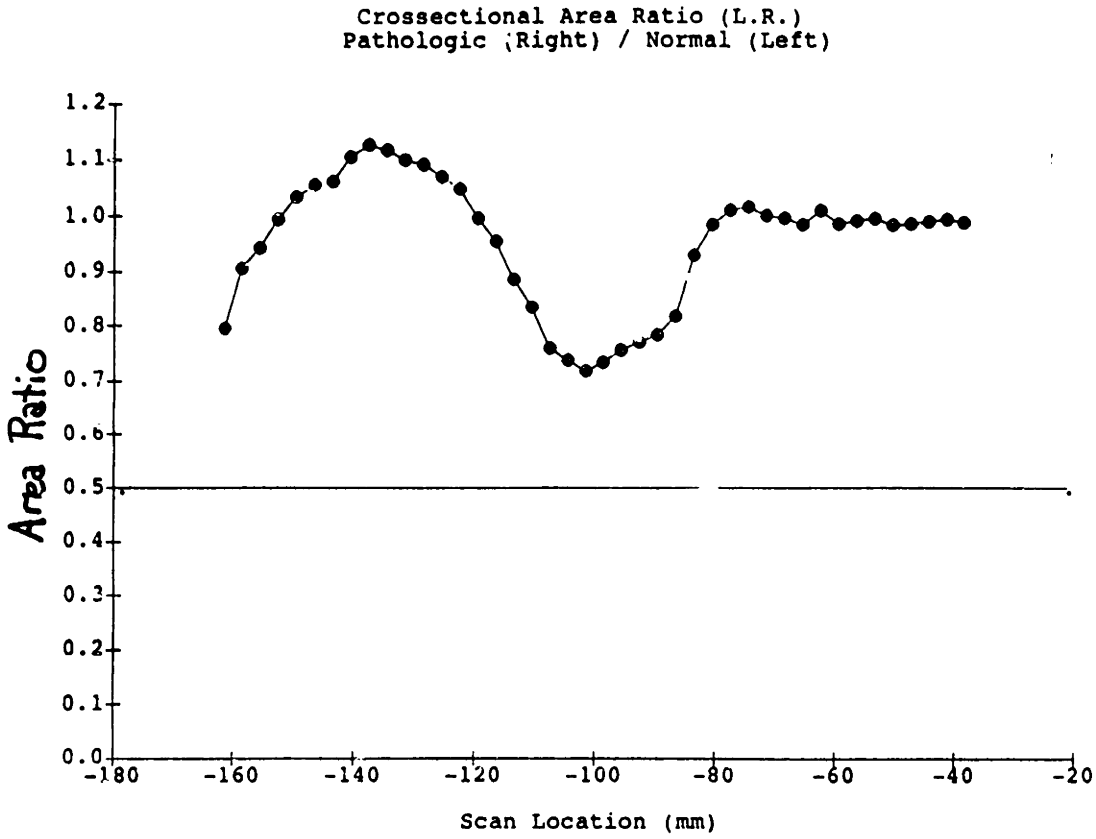

Figure 3-3: Change in crossectional area ratio with scan location.

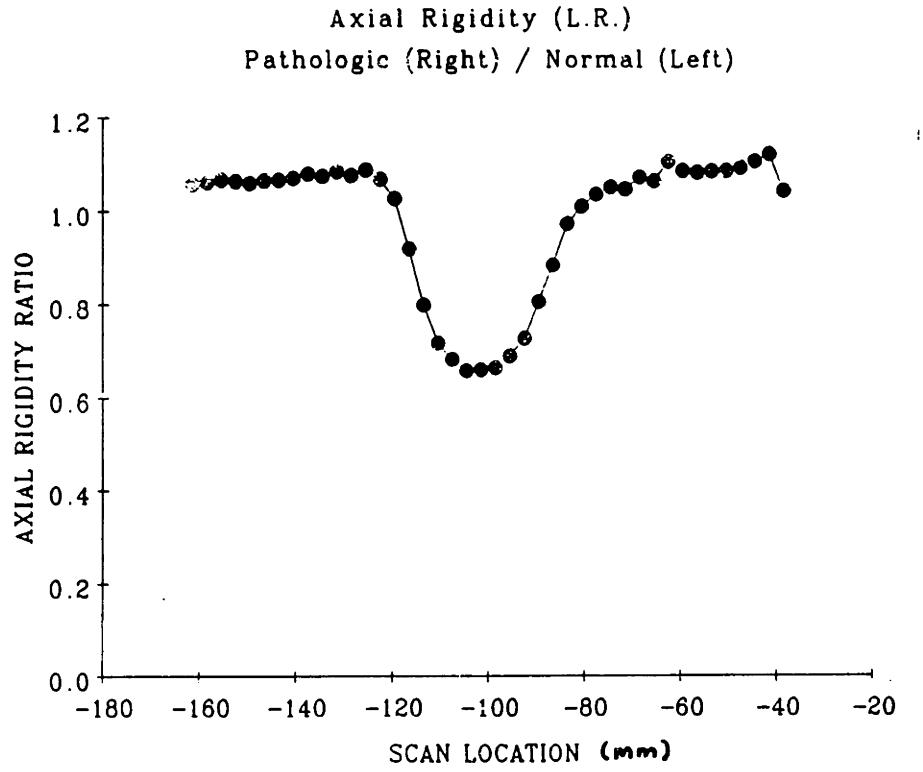

Figure 3-4: Change in axial rigidity ratio with scan location.

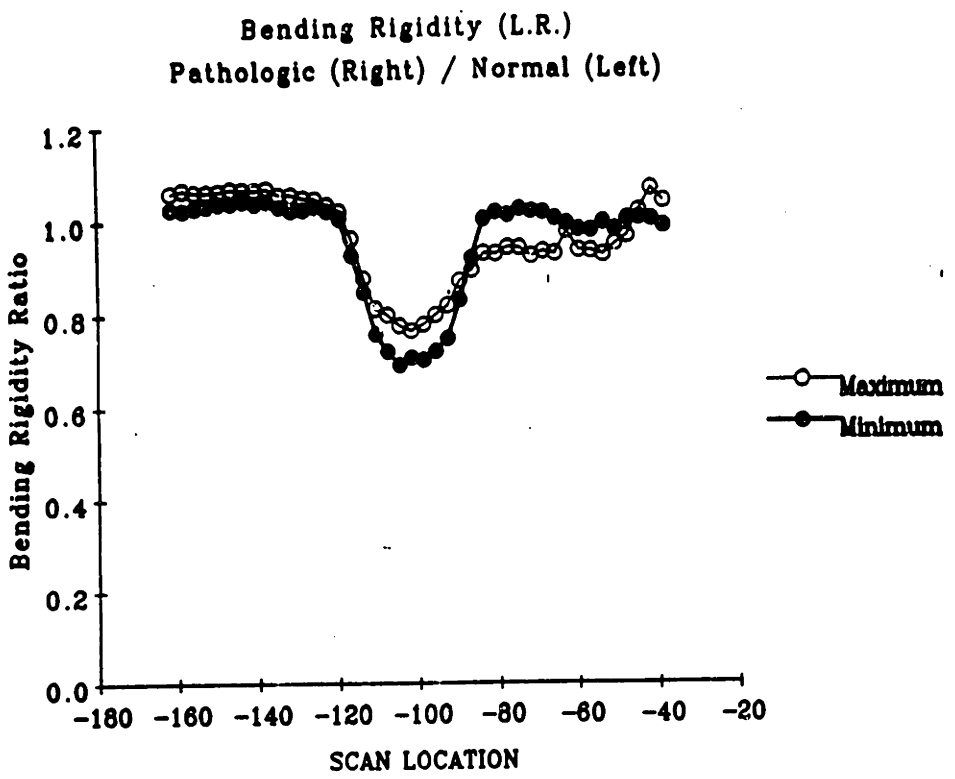

Figure 3-5: Changes in maximum and minimum bending rigidities with scan location.

shown in Figure 3-6 where the minimums are expressed as percentages of the normal contralateral side.

3.2 Comparison of Strength Reductions with Experimental Results

As described previously, patient A.B. had an endosteal defect located in the diaphysis of the left femur. This particular section of the bone most closely approximates a tube in shape and therefore is most amenable to engineering-type analysis. In the study of endosteal defects conducted by Hipp, et al. [16], a finite element model was found to predict the percentage intact strength for endosteal defects fairly well as a function of the percentage of intact crossectional area. Figure 3-7 shows the graph they obtained, along with data points added for the patient A.B. The graph shows that the beam theory analysis used in the present study also generally agrees with the experimental data. The value for the minimum bending rigidity lies directly on the linear regression line; however, the maximum bending rigidity value lies approximately 10% above the

Minimum Geometric and Strength Values for Defects
(Expressed as percentages of values for normal contralateral bone)

PATIENT	CROSSECTIONAL AREA	DENSITY	MODULUS	AXIAL RIGIDITY	MAX BENDING RIGIDITY	MIN BENDING RIGIDITY
A.B.	92%	88%	85%	92%	108%	88%
E.B.	104%	82%	49%	67%	73%	69%
C.D.	82%	75%	46%	54%	53%	47%
D.J.	88%	86%	60%	74%	89%	84%
G.L.	92%	79%	51%	59%	45%	47%
J.L.	114%	74%	44%	65%	61%	59%
K.M.	91%	107%	108%	108%	109%	122%
V.M.	88%	70%	61%	66%	51%	69%
L.P.	98%	75%	44%	55%	48%	60%
J.P.	118%	76%	39%	57%	92%	102%
L.R.	72%	87%	77%	66%	57%	69%
M.S.	92%	87%	74%	78%	69%	79%
P.S.	59%	76%	42%	55%	42%	29%
MEAN	92%	82%	60%	69%	69%	71%
ST DEV	16%	10%	21%	16%	23%	25%

Figure 3-6: Table of minimum values for properties in the regions of the defects, expressed as percentages of contralateral bone.

upper 95% confidence interval.

3.3 Non-correlation Between Cortical Area and Strength

In order to discover if there was any correlation between reduction in crossectional area and reduction in strength which is valid for all types of defects (as the current guidelines presume to be), a plot was made similar to Figure 3-7 from the cases presented in this study using the data in Figure 3-6 (See Figure 3-8). In order to prove a correlation between the two parameters, linear regressions were performed for each of the three rigidities, along with goodness-of-fit statistics. No statistically significant correlation was found between percentage of area remaining and any of the rigidity measures since all regressions yielded significance levels (p-values) much greater than 0.05. (Refer to Figure 3-8 for significance levels and R^2 values.)

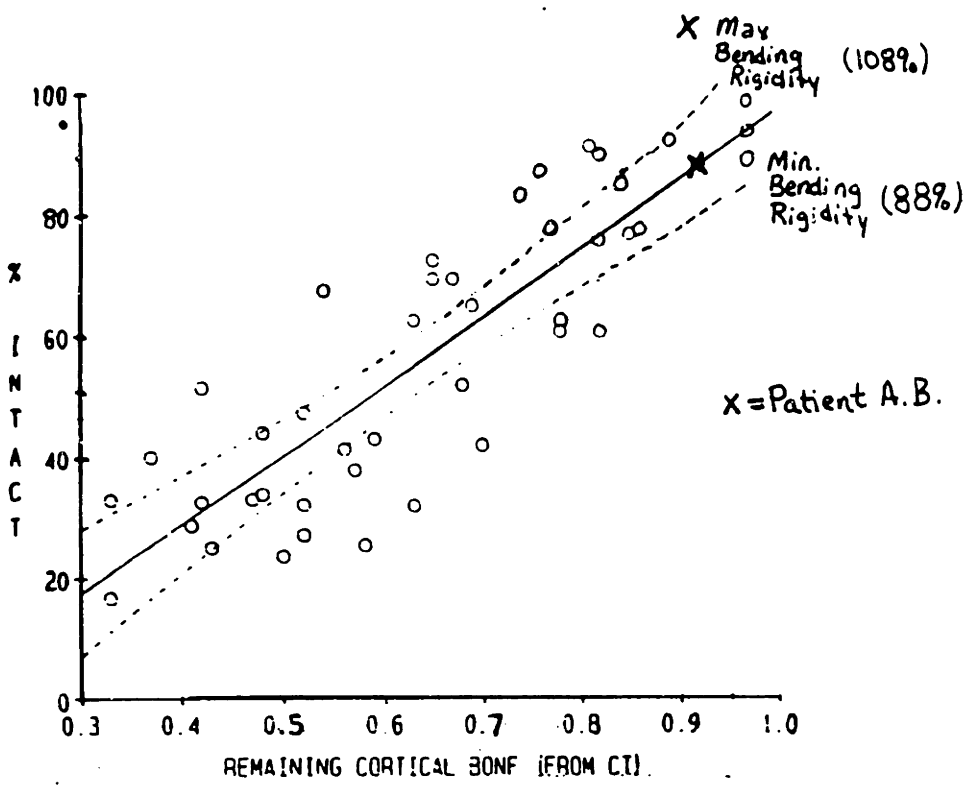

Figure 3-7: Percent intact strength as a function of percent cortical area remaining (determined by CT). (Adapted from Hipp et al., 1989 [16])(Refer to Figure 2-8.)

3.4 Clinical Use of 50% Cortical Loss Guideline

Additional information can be drawn from the minimum crossectional area, density, modulus, and strength (rigidity) values. For all thirteen patients who had been determined by a clinician to have a defect posing an "impending fracture", the mean of the percent remaining crossectional area was 93% (SD = 15%), well above the 50% guideline (43% above). The lowest value for remaining cortical area out of all the cases was 59%, still above the criteria value. The average density and modulus percentages were 81% and 59%, respectively. The average percentages for remaining strength (axial and maximum/minimum bending) were all approximately 70%.

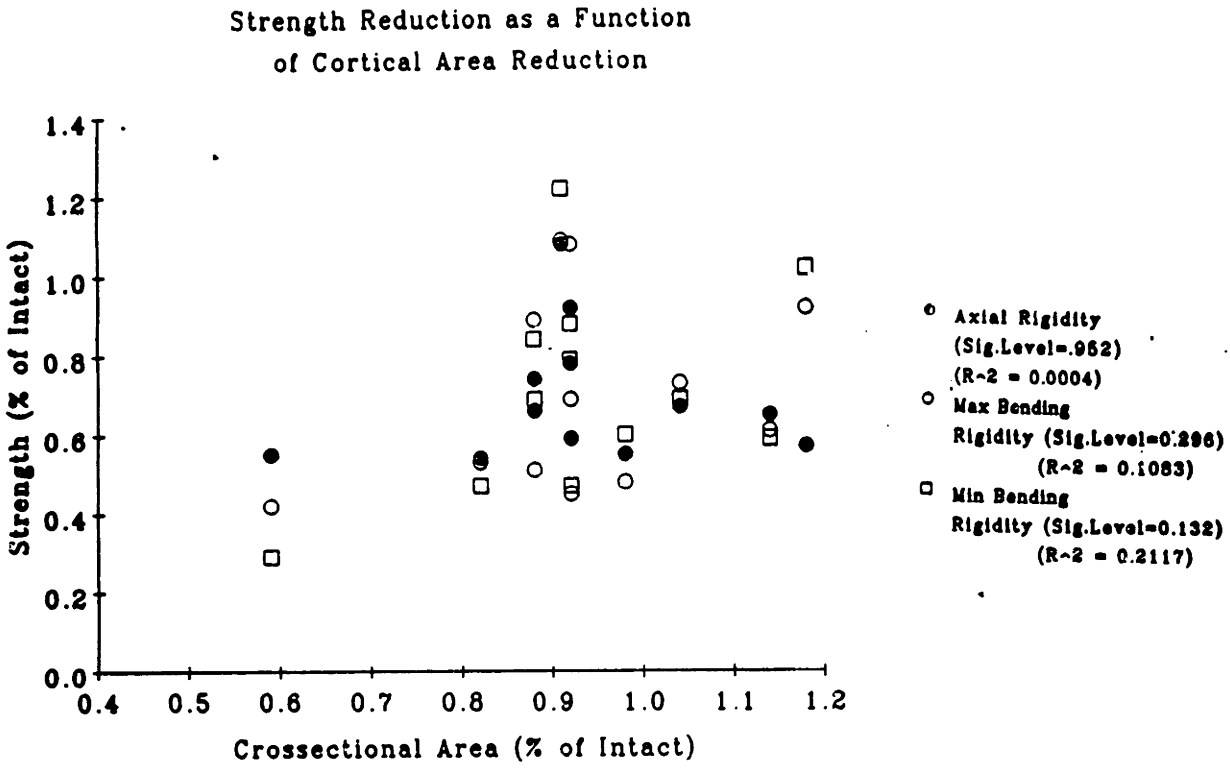

Figure 3-8: Percent intact strength as a function of percent crossectional area remaining (determined by CT). No statistiscally significant correlation was found between the percentage of area remaining and any of the rigidity measures.

Chapter 4

Discussion

4.1 Limitations of Biomechanical Analysis

The following limitations of the biomechanical analysis must be considered when interpreting this data:

1) The structural "safety factor" present in a normal femur is not known. Therefore, it is not possible to determine whether a pathologic fracture is likely from only the stated geometrical changes and strength reductions.

2) The composite beam theory analysis used in the analysis does not account for stress concentration factors around the lesion and thus tends to underestimate the strength reductions.

3) The lesion may cause mechanical property alterations in bone juxtaposed to the lesion even though the changes are not radiographically evident. These possible changes have not yet been documented and, if present, would most likely increase the strength reductions.

4.2 Comparison with Prior Experimental Results

In Figure 3-7, it was seen that the minimum bending rigidity prediction for patient A.B. was within the accepted confidence interval, but that the maximum rigidity value was well above it. This result is compatible with what is known about the

composite beam theory analysis: it tends to underestimate the strength reductions (hence, overestimating the remaining fraction of intact strength) since it does not account for stress concentration factors [21, 16]. It should be recognized though, that this result is quite good considering that the defect was by no means as "ideal" as the ones which were created in the canine femora for the experiments.

The value of 108% for the maximum bending rigidity percentage is worth noting. It shows that the strength in the area of the lesion may be higher than normal even though there was an 8% reduction in crossectional area. This calls attention to the fact that other factors, especially density/modulus, are not insignificant and should be included in the criteria for determining impending fracture. This is also evident in the case of J.L., where the strength is reduced to an average of 61% even though the crossectional area at the defect is 14% greater than normal.

Chapter 5

Conclusions and Recommendations

All four of the objectives for assessing the 50% cortical loss guideline were accomplished. From the literature, it was noted that the qualitative criteria was not scientifically validated and that following it rigorously would allow substantial strength reduction to occur; higher than what would be considered "acceptable" fracture risk. Even though little is known about safety factors for loaded bones, the tremendous reductions in strength (80-90% for transcortical defects, 60-70% for endosteal) which would result from following the criteria should be considered hazardous, since it is common to exceed normal bone loading by many times more than a factor of two. It is also unknown how much conditions such as osteoporosis reduce the safety margin.

In addition, it was demonstrated that there was no universal correlation betweeen crossectional area and strength for the cases considered in this study. If such a cortical loss criterion is to be defined, it will most likely need to be different for each type of lesion or location, such as the experimentally determined relationship for endosteal, diaphyseal defects. In addition, it is difficult to justify the prediction of strength from crossectional area ratio only since the density and modulus of the bone are such significant factors. This was emphasized by the two patients, A.B. and J.L., mentioned in the discussion.

Finally, the high mean value of 93% for the average crossectional area of the cases

in this study leads to the conclusion that the 50% cortical loss criterion was not a significant factor in the clinical assessment of their lesions. This is understandable since the measurement of cortical area loss from plane radiographs is complicated, not very accurate, and depends greatly on proper orientation. Even when computed tomography is used, the measurement is still not simple or available enough to be popular. In addition, since there was never very substantial support for the criterion in the first place, it does not seem to merit the additional effort.

From all this, it seems reasonable to conclude that the 50% cortical area loss criterion is unsubstantiated, inappropriate, hazardous, and impractical. However, this leads to the question of what guidelines should replace it? The most suitable guidelines would include several factors of importance such as degree of pain, reduction in mechanical strength, level of activity, and expected survival time. For some patients, a purely strength reduction-based criterion, although very scientific, would not lead to the most beneficial assessment of their condition. For example, if a patient's level of activity is low, the reduction in bone strength may be of little consequence and surgical stabilization of the defect would be unnecessary trauma. In the opinion of one of the collaborating surgeons, too many patients are being operated on unnecessarily due to the lack of objective guidelines. He predicts that only 2 or 3 out of 10 patients who undergo stabilization would actually have sustained a pathological fracture without the operation. If true, this would mean that about two-thirds of the current fixation surgeries are potentially unnecessary, possibly because the strength reduction is not very great or the patient's level of activity is so low that the bone would never be loaded enough for fracture. Because there are no proven guidelines however, the clinicians must decide conservatively. Hence, the substantial need for guidelines which can predict impending fracture, but can also determine when surgery is unnecessary or not beneficial.

In order to establish a new set of such objective guidelines, further research is still required. This was a study with a small group of similar cases. Establishing guidelines will take a much larger number of these case analyses for several types of defects. To this end, more should be done in categorizing defects along with their

characteristics; there is such a wide range of lesion types that it seems the number of groups will be quite formidable.

Another recommendation is for new retrospective studies of pathological fractures which were due to metastatic disease. With the more advanced analysis techniques available, perhaps more could be learned from them now than previously. The analysis techniques should also be improved to more closely model bone and also to attempt to incorporate the quality of the bone surrounding the defect. Recent progress in complex finite element modelling appears promising.

Appendix A: Patient Population

PATIENT	SEX	AGE	PRIMARY CANCER	LESION	
A.B.	Female		Breast	Left, diaphysis	Endosteal cortical lesions
E.B.	Female	78	Breast	Right, proximal	
C.D.	Female	30	Breast	Right, proximal	Mixed lytic and sclerotic processes
D.J.	Male	5		Left, distal metaphysis	Non-ossifying fibroma
G.L.	Male	9		Right,	Fibrous dyphasic lesion
J.L.	Female	72		Right,	
K.M.	Female	15		Right, distal metaphysis	Non-ossifying fibroma
V.M.	Male	61	Renal cell carcinoma	Left, proximal	Endosteal cortical lesions
L.P.	Male	27	Malignant desmoplastic small cell tumor	Left, proximal shaft	
J.P.	Male	51	Enchondroma	Left, proximal	Mixed lytic/blastic, confined to trabecular
L.R.	Male	77		Right, diaphysis	
M.S.	Female	60		Right, proximal	
P.S.	Female	58		Left, proximal	Calcar, lesser trochanter

MEAN		45			
ST DEV		27			

Bibliography

[1] H. Altman. Intramedullary nailing for pathological and impending fractures of long bones. *Bulletin of the Hospital for Joint Diseases Orthopaedic Institute*, 13:239–251, 1952.

[2] R.K. Beals, G.D. Lawton, and W.E. Snell. Prophylactic internal fixation of the femur in metastatic breast cancer. *Cancer*, 28:1350–1354, 1971.

[3] C.O. Bechtol. *'Bone as a structure.' In: Metals and Engineering in Bone and Joint Surgery.* Williams and Wilkins Company, Baltimore, MD, 1959.

[4] D.B. Brooks, A.H. Burstein, and V.H. Frankel. The biomechanics of torsional fractures: the stress concentration effect of a drill hole. *Journal of Bone and Joint Surgery*, 52:507–514, 1970.

[5] D.R. Carter and W.C. Hayes. The compressive behavior of bone as a two-phase porous structure. *Journal of Bone and Joint Surgery*, 59 A:954–962, 1977.

[6] E.Y.S. Chao, F.H. Sim, T.C. Shives, and D.J. Pritchard. *'Management of pathologic fracture: Biomechanical considerations.' In: Diagnosis and Management of Metastatic Bone Disease.* Raven Press, New York, NY, 1988.

[7] C.R. Clark, C. Morgan, D.A. Sonstegard, and L.S. Matthews. The effect of biopsy-hole shape and size on bone strength. *Journal of Bone and Joint Surgery*, 59:213–217, 1977.

[8] M. Fidler. Prophylactic internal fixation of secondary neoplastic deposits in long bones. *British Medical Journal*, 1:341–343, 1973.

[9] V.H. Frankel, A.H. Burstein, and (ed. Kenedi RM). *'Load capacity of tubular bone.' In: Biomechanics and Related Bio-Engineering Topics.* Pergamon Press, Oxford, England, 1965.

[10] F.J. Frassica, F.H. Simm, and (ed. F.H. Simm). *Pathogenesis and Prognosis In: Diagnosis and Management of Metastatic Bone Disease.* Raven Press, New York, NY, 1988.

[11] H.K. Genant, J.S. Wilson, and et al. Computed tomography of the musculoskeletal system. *The Journal of Bone and Joint Surgery*, 62-A(7):1088–1101, October 1980.

[12] K.D. Harrington. Metastatic disease of the spine. *Journal of Bone and Joint Surgery*, 68-A:1110–1115, 1986.

[13] K.D. Harrington. *Orthopaedic Management of Metastatic Bone Disease.* The C. V. Mosby Company, St. Louis, MO, 1988.

[14] J.A. Hipp, E.J. Cheal, and W.C. Hayes. *'Biomechanics of Fractures.' In: Skeletal Trauma.* (eds. B. Browner, J. Jupiter and A. Levine) W.B. Saunders Company (in press), 1991.

[15] J.A. Hipp and W.C. Hayes. Structural consequences of transcortical holes in long bones loaded in torsion. *Journal of Biomechanical Engineering*, 1988.

[16] J.A. Hipp, R.J. McBroom, E.J. Cheal, and W.C. Hayes. Structural consequences of endosteal metastatic lesions in long bones. *Journal of Orthopaedic Research*, 7:828–837, 1989.

[17] R.E. Leggon, R.W. Lindsey, and M.M. Panjabi. Strength reduction and the effects of treatments of long bones with diaphyseal defects involving 50% of the cortex. *Journal of Orthopaedic Research*, 6:540–546, 1988.

[18] M. Lenz and J.R. Freid. Metastases to the skeleton, brain, and spinal cord from cancer of the breast and the effect of radiotherapy. *American Journal of Surgery*, 93:278–293, 1931.

[19] R.P. Lewallen, D.J. Pritchard, and F.H. Sim. Treatment of pathologic fractures or impending fractures of the humerus with rush rods and methylmethacrylate. *Clinical Orthopaedics and Related Research*, pages 193–198, 1982.

[20] P. Manch, M. Drew, (eds. V. DeVita, S. Hellman, and S. Rosenberg). *'Treatment of metastatic cancer to bone.' In: Cancer:Principles and Practice of Oncology.* JB Lippincott Co., Philadelphia, PA, 1985.

[21] R.J. McBroom, Cheal E.J., and W.C. Hayes. Strength reductions from metastatic cortical defects in long bones. *Journal of Orthopaedic Research*, 6(3):369–378, 1988.

[22] R.J. McBroom and W.C. Hayes. Strength reduction and fracture risk of cortical defects in the diaphysis of long bones. *Trans. 30th Annu. Meet. Orthop. Res. Soc.*, 9:320, 1984.

[23] R.J. McBroom, W.C. Hayes, and P. Poon. Strength reduction of endosteal defects in diaphyseal bone. *Trans. 32nd Annu. Meet. Orthop. Res. Soc.*, 11:65, 1986.

[24] G.V. Miller, R.A. VanderGriend, P. Blake, and D.S. Springfield. Performance evaluation of a cement augmented intramedullary fixation system for pathological lesions of the femoral shaft. *Clinical Orthopaedics and Related Research*, 221:246–254, 1987.

[25] R.M. Rivello. *Theory and Analysis of Flight Structures.* McGraw-Hill, New York, NY, 1969.

[26] M.M. Sherry, F.A. Greco, and D.H. Johnson. Metastatic breast cancer confined to the skeletal system. *American Journal of Medicine*, 81:381–386, 1986.

[27] E. Silverberg and J. Lubera. Cancer statistics, 1986. *Cancer*, 36:9–25, 1986.

[28] F.H. Sim and D.J. Pritchard. Metastatic disease in the upper extremity. *Clinical Orthopaedics and Related Research*, pages 83–94, 1982.

[29] R.M. Wilkins and F.H. Sim. *'Lesions of the femur.' In: Diagnosis and Management of Metastatic Bone Disease.* Raven Press, New York, NY, 1986.